# Wavelength and shape dependent strong-field photoemission from silver nanotips

Mina Bionta, Sébastien J. Weber, Ivan Blum, Julien Mauchain, Béatrice Chatel, Benoît Chalopin

IOP Publishing New J. Phys. 18 (2016) 103010 doi:10.1088/1367-2630/18/10/103010

New Journal of Physics
The open access journal at the forefront of physics

Deutsche Physikalische Gesellschaft DPG
IOP Institute of Physics

Published in partnership with: Deutsche Physikalische Gesellschaft and the Institute of Physics

PAPER

# Wavelength and shape dependent strong-field photoemission from silver nanotips

M R Bionta[1,4], S J Weber[1,2], I Blum[3], J Mauchain[1], B Chatel[1] and B Chalopin[1]

[1] LCAR-UMR 5589-Université Paul Sabatier Toulouse III-CNRS, 118 Route de Narbonne, Bat 3R1B4, F-31062 Toulouse Cedex 9, France
[2] CEMES—CNRS, 29 rue Jeanne Marvig, F-31055 Toulouse, France
[3] GPM, UMR 6634 Université de Rouen-CNRS, Avenue de l'Université, BP 12, F-76801 St Etienne du Rouvray, France
[4] Current Address: Institut national de la recherche scientifique, Centre-Énergie, Matériaux et Télécommunications, 1650 Blvd. Lionel-Boulet, Varennes, QC J3X 1S2, Canada.

E-mail: benoit.chalopin@irsamc.ups-tlse.fr

Keywords: nanotip, photoemission, strong-field, plasmon

OPEN ACCESS

RECEIVED
20 July 2016

REVISED
30 August 2016

ACCEPTED FOR PUBLICATION
19 September 2016

PUBLISHED
7 October 2016



## Abstract

We study optical field emission from silver nanotips, showing the combined influence of the illumination wavelength and the exact shape of the nanotip on the strong-field response. This is particularly relevant in the case of FIB milled nano tips, where the nanotip fabrication capabilities could become a new ingredient for the study of strong-field physics. The influence of the thermal load on the nanotip and its effect on the emission is studied as well by switching the repetition rate of the laser source from 1 kHz to 62 MHz, showing a clear transition towards the quenching of the strong-field emission.

## 1. Introduction

The interaction of intense ultrashort laser pulses and metallic nanotips offers the possibility of a strong confinement of the electromagnetic field in both time and space [1, 2], on the sub-femtosecond and nanometer scales. It has led to the observation of electron emission from multiphotonic processes as well as strong-field behavior similar to that in atoms and molecules [3–5]. Moreover, this interaction allows the production of electron wave packets [6], and opens the route to ultrafast time resolved electronic microscopy and diffraction studies [7–9]. Nanotips have several advantages compared to bulk or gas phase systems because the electron confinement and plasmonic response increase the local electric field at the tip apex. In this regard, the tip material and its shape play a major role in this interaction. Many studies have been done with tungsten tips [1, 3, 6, 8, 10, 11] as it is is a robust material with a high melting point, and tips are easy to produce. In the visible range however, tungsten has a weak plasmonic response and the field enhancement is mostly due to the charge confinement at the apex. Gold is a plasmonic metal that is also vastly used [2, 12] which exhibits higher field enhancement due to the large value of its dielectric permittivity (with negative real part). More exotic materials have also been investigated, such as hafnium carbide nanotips [13] because of its low work function, and carbon cone nanotips [14] that have remarkable cold field emission properties. Silicon nanotips have also been used as optical field emitters arrays [15]. In this paper we will present new results obtained from silver nanotips. These tips have been used for scanning optical tunneling microscope where they have shown higher luminescence intensities than tungsten [16], but have been barely used for laser-induced photoemission [17]. Silver's plasmonic properties are strongest in the visible range, but are accompanied by a lower melting point leading to potential thermal issues and a more complex fabrication process. We demonstrate first the optical field emission and the characterization of the nanotip field enhancement at 800 and 400 nm, with surprising results confirmed by numerical calculation of the electric field enhancement for the specific tip shape used in the experiment. This strong field behavior disappears when using a high repetition rate laser source (high mean power), which suggests that thermal effects in the nanotip suppress or at least modify the photoemission characteristics.

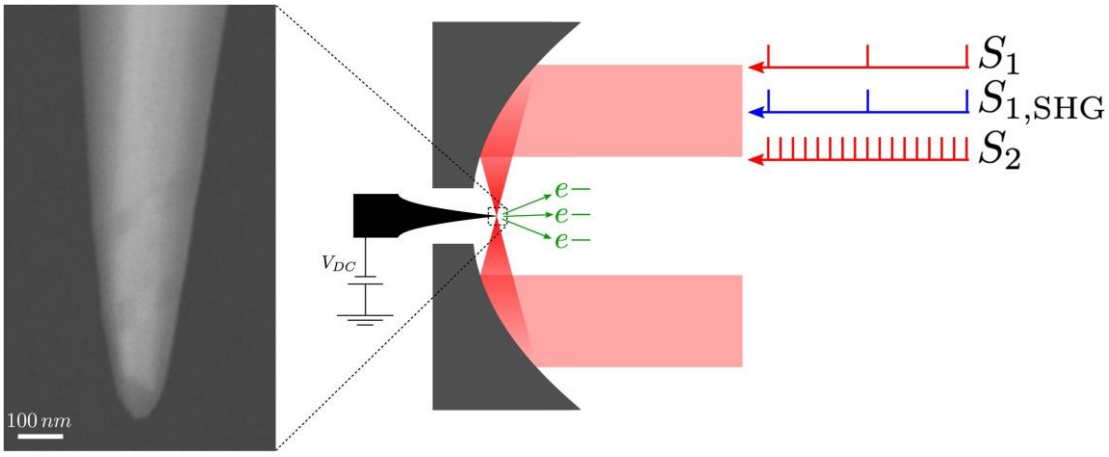


Figure 1. SEM picture of the FIB-milled silver nanotip and sketch of the experimental setup: different femtosecond laser sources are focused on the silver nanotip and the kinetic energy spectra of the emitted electrons are recorded. Source $S_1$ produces ultrashort pulses (< 30 fs) at 800 nm with a low repetition rate (1 kHz). $S_{1,\mathrm{SHG}}$ is the second harmonic of source $S_1$ giving similar pulses at 400 nm. $S_2$ gives the same pulses than $S_1$ with a larger repetition rate (62 MHz).

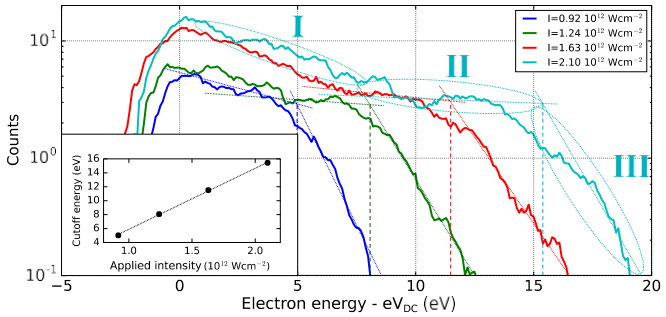


Figure 2. A series of photoemission spectra obtained with increasing laser intensity at 1 kHz repetition rate at 800 nm ($S_1$). The $x$ axis represents the measured energy minus the energy from the tip bias $eV_{DC}$. The colored dashed lines are the linear asymptotes from which the cutoffs have been extracted. The inset shows the evolution of the cutoff energy position, defined as the intersection of the dashed lines, as a function of applied laser intensity using $S_1$. The dashed line is a linear fit with a slope of 8.8 × $10^{-12}$ eV (W cm$^{-2}$)$^{-1}$.

## 2. Experimental setup

Silver nanotips are made using both electrochemical etching and focused ion beam (FIB) annular milling as in [17, 18]. Figure 1 shows the nanotip used in this experiment after the FIB milling process. More experimental details on the fabrication process can be found in appendix A.

The photoemission experimental setup is depicted briefly in figure 1 and is detailed in appendix B. It uses two laser sources ($S_1$ and $S_2$) at 800 nm with 20−30 fs duration that have different repetition rates as well as the second harmonic generation of source $S_1$. The tip is biased with a moderate voltage $V_{DC}$ to accelerate electrons towards the detector. Laser pulses are tightly focused on the nanotip with off-axis parabolic mirrors and the kinetic energy spectrum of emitted electrons is recorded with a retarding field spectrometer.

## 3. Strong *fi*eld photoemission and optical *fi*eld enhancement

Figure 2 shows photoelectron spectra in semilog scale recorded with source $S_1$ for different laser intensities in which we determine the kinetic energy acquired for the emitted electrons with respect to the applied tip bias. These spectra are very broad and present features typical of optical field emission. This is the first demonstration of strong-field behavior from silver nanotips. The spectra extend into the 10−15 eV range, way above the expected above threshold emission energy for multiphotonic emission. Three regions are visible: (I) at low energy, the spectrum decreases exponentially as expected from multiphoton emission, (II) the yield becomes quasi constant forming a 'plateau' region, (III) finally the emission yield rapidly decreases until the 'cutoff'. This is a clear observation of strong field emission and elastic scattering well known in atoms and molecules [19].

Table 1. Applied laser intensities and retrieved cutoff energies and intensity enhancement.

| Applied intensity ($10^{12}$ Wcm$^{-2}$) | Calculated $E^{cut}$ (eV) | Measured $E^{cut}$ (eV) | Effective intensity ($10^{12}$ Wcm$^{-2}$) | Keldysh parameter $\gamma$ | Intensity enhancement $h^{I}$ |
|---|---|---|---|---|---|
| 0.92 | 0.549 | 7.92 | 13.24 | 1.64 | 14.42 |
| 1.24 | 0.739 | 11.01 | 18.47 | 1.39 | 14.90 |
| 1.63 | 0.976 | 14.42 | 24.08 | 1.22 | 14.78 |
| 2.1 | 1.255 | 18.33 | 30.67 | 1.08 | 14.60 |

Emitted electrons are accelerated by the laser electric field and return to the metal-vacuum interface. A possible outcome of this recollision process is elastic backscattering. These electrons can then acquire more kinetic energy as they are further accelerated by the electric field. This translates into the observed plateau in the energy spectrum, with a maximum energy, the 'cutoff', given by the following expression:

$$E^{cut} \gg 10\, U_p = 10\, \frac{e^2}{2e_0 m_e}\, \frac{I^{loc}}{w^2}, \tag{1}$$

where $U_p$ is the ponderomotive energy, $I^{loc}$ the local intensity at the metal surface, $w = 2p\frac{c}{\lambda}$ the optical angular frequency with $\lambda$ the central wavelength, $e$ the electron charge, $e_0$ the permittivity of free space, $m_e$ the electron mass, and $c$ the speed of light in vacuum. Measuring $E^{cut}$ allows us to calculate the *in situ* optical intensity $I^{loc}$. This expression is valid as long as the electric field can be considered homogenous along the electron trajectory which we confirmed *a posteriori* using the argument developped in [4]. The cutoff position can be extracted from the spectra using the intersection of the linear curves fitting both regions II and III [20, 21]. For each curve in figure 2, the cutoff position has been extracted at the intersection of the fits. The energy extension of the spectra closely follows the laser intensity as shown in the inset where cutoff energies are plotted as a function of incident laser intensities. The cutoff varies linearly with intensity accordingly to equation (1). This clearly demonstrates the strong field recollision regime reached here with silver nanotips. Moreover, the local intensity can be determined using equation (1) and the experimental intensity enhancement can be calculated, using the method of [21].

A linear fit of the cutoff position with respect to the intensity shows an offset of about −2.94 eV. We attributed this to the geometrical alignment of the tip with respect to the spectrometer: if the electrons enter the spectrometer with an angle, the static field correction of the spectrum detailed above is overestimated. This defines the zero-energy point of the photoemission spectrum. Therefore, before deriving the local intensity, the cutoff values are corrected with this offset. Table 1 summarizes the parameters used: measured and corrected cutoff values and derived intensity enhancement factor $h^{I}$. This factor is defined as the ratio between local intensity (or effective intensity) at the tip apex and the applied intensity calculated from the energy, duration and focus size of the laser pulse. We also calculated the Keldysh parameter $g = \sqrt{\frac{f}{2U_p}}$ assuming the workfunction of silver to be $f = 4.26$ eV.

$$h^{I} = \frac{\text{Effective intensity}}{\text{Applied intensity}} = \frac{\text{Measured } E^{cut}}{\text{Calculated } E^{cut}}. \tag{2}$$

On average, the intensity enhancement is on the order of 14.5, corresponding to an electric field enhancement $x = \sqrt{h^{I}} = 3.8 \pm 0.1$. This enhancement is both due to the local electron confinement and the plasmonic behavior of the metal, each depending on the tip shape. The first effect is present for all nanotips including tungsten which is not plasmonic in the visible/near IR range. However, due to the high plasmon response of silver in the visible wavelengths, it is of interest to study its strong field behavior as a function of wavelength, leading to possibly high energy electrons with limited laser power.

The same experiments were performed at 400 nm using the second harmonic of Source $S_1$ generated inside a 250 $\mu$m thick Beta Barium Borate crystal ($BaB_2O_4$ or BBO). Figure 3 shows the spectra obtained at 400 nm compared with those for 800 nm with same pulse energy. The ponderomotive energy and therefore the cutoff scales as $I^2$, so that one can expect the spectra to be narrower for 400 nm compared to 800 nm. However, this is not the case. The spectra are broader at the shorter wavelength, which clearly indicates that the local intensity at the metal interface is higher at 400 nm, proving another important difference with what can be achieved with atomic strong-field physics. We repeated the same procedure to calculate the intensity enhancement in this case. However, we could not get a precise value for the applied intensity because the pulse duration and focus size could not be precisely measured. Nonetheless, if we assume the same pulse duration and the same focus size for both wavelengths, a conservative estimate, we find an intensity enhancement for 400 nm on the order of 150, corresponding to a field enhancement of $\sim 12.2 \pm 2$, considerably higher than found for 800 nm. This behavior

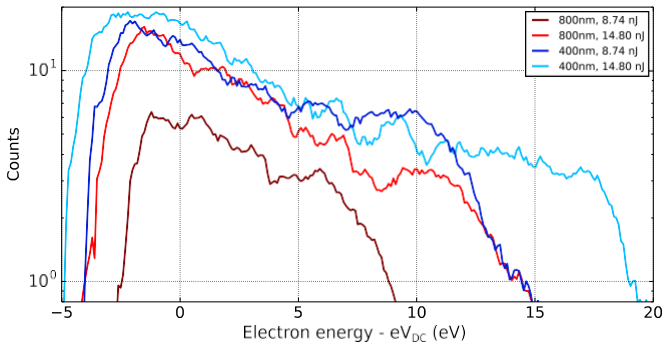


Figure 3. Comparison between silver photoemission spectra using 800 nm (red and brown) and 400 nm (light and dark blue) laser pulses with comparable pulse energies and therefore similar intensities.

is unexpected as one expects the field enhancement to be higher at 800 nm due to the larger ratio between wavelength and tip radius, as well as the larger value of the dielectric permittivity [22, 23].

## 4. Numerical calculation of the *field* enhancement with optimized tip shapes

The plasmonic behavior of nanostructures depends on the material through the dielectric permittivity , its shape and the illumination wavelength. For conical nanotips with a small radius, it has been demonstrated that there is a cone angle that gives the highest electric field enhancement [24], the resonant angle $\alpha$ being given by:

$$\alpha = \arccos\left(\frac{\mathrm{Re}(\quad) + 1}{\mathrm{Re}(\quad) - 1}\right). \tag{3}$$

The dielectric permittivity of silver varies greatly between 800 nm and 400 nm wavelengths, as such the resonant angle varies from 20° at 800 nm to 50° at 400 nm. This means that a large opening angle would give our silver nanotip a higher field enhancement at 400 nm than at 800 nm. The silver nanotip we used, depicted in figure 1, looks sharp with a small opening angle. However, a closer look at the tip apex reveals that the shape of the apex is more complex than a regular cone. In order to understand how this shape would affect the field enhancement, we calculated numerically the field enhancement for the specific tip shape we are using. We used COMSOL Multiphysics software to model the nanotip and compute the local field enhancement with the following values from [22] for the dielectric permittivity of silver for the wavelengths modeled:

$$_{\mathrm{Ag},800} = -27.93 + 1.5222i, \tag{4}$$

$$_{\mathrm{Ag},400} = -3.7726 + 0.6747i. \tag{5}$$

Maxwell's equations were solved in the frequency domain using matched layers that absorbed the propagating plasmons at the wall of the simulation box. This prevents plasmons from getting reflected at the border of the simulation box. This method allowed us to reproduce results for conical-shaped tips such as those modeled in [24, 25] that were computed using other methods. Since the absolute value of is greater at 800 nm than at 400 nm, one expects the field enhancement to be larger at 800 nm, contrary to what was measured experimentally. From the SEM image of the silver nanotip, we noticed that even though the cone angle seems small far from the apex, it increases a lot close to the apex. To account for this effect in our case, we modeled the silver nanotip (figure 4(a)) with a two-angle cone with half opening angles $\alpha_1 = 33$ and $\alpha_2 = 10$ terminated by a spherical apex of radius $r = 20$ nm with a distance $h_1 = 64$ nm between the apex and the start of the second cone. These numerical values are directly extracted from a SEM image of the nanotip.

Figure 4(b) represents the value of the electric field versus distance from the tip surface along the line where it is maximum. We found that indeed the field enhancement at 400 nm ($x_{400} \gg 7.7$) is greater than that at 800 nm ($x_{800} \gg 6.3$). While these values do not correspond exactly to those retrieved experimentally, they show the same general trend in regards to wavelength dependency, and thus with more accurate modeling of the nanotip, could give values closer to those found. We can see that the field enhancement at 400 nm is confirmed to be higher than that at 800 nm. When modeling the nanotip with the typical conical shape found in literature, with a half-angle equal to 10, the results are drastically different with field enhancement equal to 2.4 at 400 nm and 6.8 at 800 nm.This means that in the case of a two-angle conical nanotip, the exact value of the field at the apex is mostly depending on the tip angle near the apex.

These results are a clear demonstration of the effect of the tip shape on its plasmonic response leading to possibly higher field enhancements. This behavior is especially important in the case where the nanotip has a

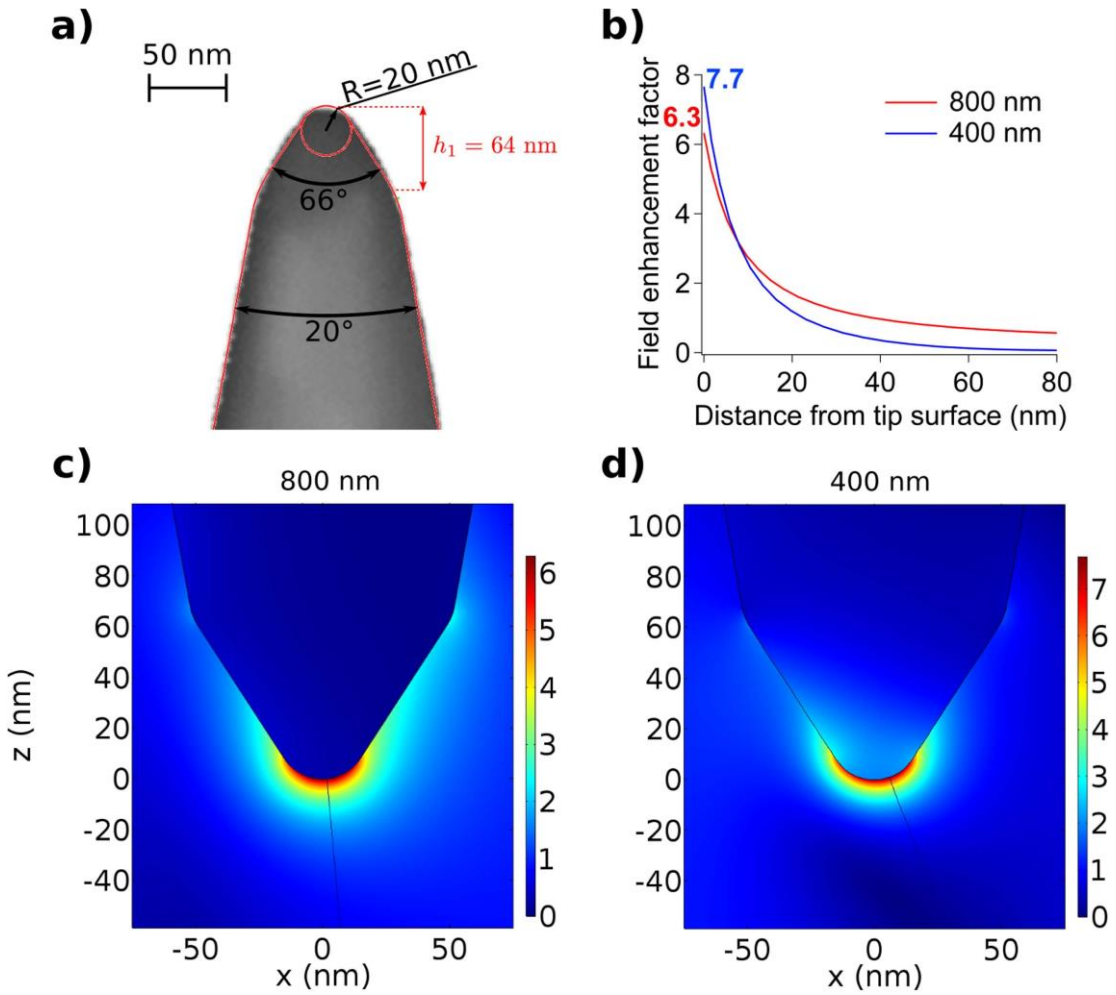


Figure 4. (a) Two-angle cone modeling of the silver nanotip from the SEM image. (b) Electric field as a function of the distance to the apex from which we extract the field enhancement. We find $\xi_{800} \approx 6.3$ and $\xi_{400} \approx 7.7$. (c) and (d) Result of finite element calculation of the electric field in V m$^{-1}$ at the apex of the two-angle nanotip for 800 and 400 nm illumination with an incident electric field equals to 1 V m$^{-1}$ at the apex, coming from the left side and with a polarization along the tip axis. The straight lines indicate the orthogonal lines along which the electric field is plotted in (b).

more complex shape than a typical conical one and shows that the exact shape of the nanotip is a crucial factor that determines the field enhancement at the apex of the nanotip. In the case of FIB milling of nanotips, it becomes possible to engineer the tip shape for specific values of field enhancement at different wavelengths. For instance, large opening angles and small apex sizes can lead to maximum field enhancement. This type of system is difficult to produce via electrochemical etching but not necessarily with the FIB milling technique.

## 5. Suppression of strong *field* photoemission at high repetition rates

We repeated the first experiments at 800 nm with source $S_2$ at a higher repetition rate of 62 MHz, but with similar optical intensities and slightly shorter pulse duration. The number of detected electrons per laser pulse is roughly the same, but the recorded energy spectra are completely different as seen in figure 5. The low repetition rate spectrum from $S_1$ is very broad and extends for more than 15 eV, whereas the high repetition-rate spectrum is narrower and only extends over a few eV, with most likely only multiphotonic or thermally emitted electrons. The only noticeable difference between these two experiments is the average power deposited on the nanotip, which scales as the repetition rate. This means that using source $S_2$, we have $6 \times 10^4$ more deposited energy that the tip has to dissipate per unit of time. This causes the tip to heat up to large temperatures, suppressing the strong-field behavior observed for lower repetition rates. These effects are reproducible. We are confident that the tip did not experience any damage as the DC field emission did not change between experiments. These results show that the laser repetition rate plays a major role in the emission mechanisms in laser-tip interaction in silver nanotips due to the mean power deposited in the tip. Similar effects were observed for carbon cone

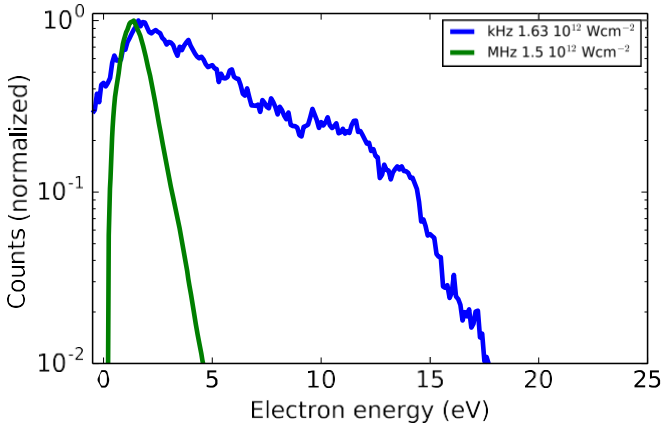


Figure 5. Electron photoemission spectra on silver nanotip with the 1 kHz $S_1$ laser source (blue) and the 62 MHz $S_2$ source (green). Both sources produce an equivalent laser intensity on the target.

nanotips [14] and led to the destruction of samples at MHz illumination, despite the mechanical stability of these tips proved in cold field emission [26]. These results ask for new variable repetition-rate tunable laser sources to investigate mean power effects on laser-induced photoemission, as well as new types of theoretical modeling to include temperature in multiphotonic and optical field emission.

## 6. Conclusion

We have presented the first observation of strong-field behavior of photoemission from silver nanotips. We have measured a stronger field enhancement at 400 nm than at 800 nm, which was confirmed by numerical calculation of the electric field on a two-angle nanotip modeled from the SEM image of the tip, proving the effect of the nanotip shape on the field enhancement, making the FIB milling process interesting for engineered tip shapes. Compared to tungsten nanotips, using silver enables plasmonic effects to play a role in electron photoemission that can therefore be controlled by an interplay of the tip shape and the field wavelength. Finally, we showed that using a high repetition rate illumination can suppress this strong field behavior due to the high mean power deposited on the nanotip. These results pave the way towards optimal control of the laser-tip interaction with more complex parameters including the tip shape and material as well as the laser repetition rate.

## Acknowledgments

We would like to thank Angela Vella and Thierry Auguste for their fruitful discussions. This work was supported by the Région Midi-Pyrénées and the Programme Investissements d'Avenir under the program ANR-11-IDEX-0002-02, reference ANR-10-LABX-0037-NEXT, and ANR-13-BS04-0007-01.

## Appendix A. Silver nanotip fabrication

The sharp silver nanotips are formed in a two-step process shown in figure A1. The tips are formed from a polycrystalline silver wire that is 99.99% pure and 125 $\mu$m in diameter. The wire is first electrochemically etched using a microloop technique [17], with a solution of 0.1% perchloric acid and 99.9% methanol and a voltage of 7 V. The tip final shape is obtained by annular milling [18] in a FIB apparatus, where the ion beam is parallel to the tip axis. The annular milling pattern is used while gradually reducing the inner radius until the correct end curvature radius is obtained. After the shape is formed, the tips are cleaned using low energy ions. In general, due to the nature of the milling process, some atoms of Ga are implanted up to $\sim$2 nm under the material surface but their influence in the emission process can be neglected. The tips have a final radius of 12–50 nm. The tip used in the following experiments is shown in figure A1 before and after the milling process.

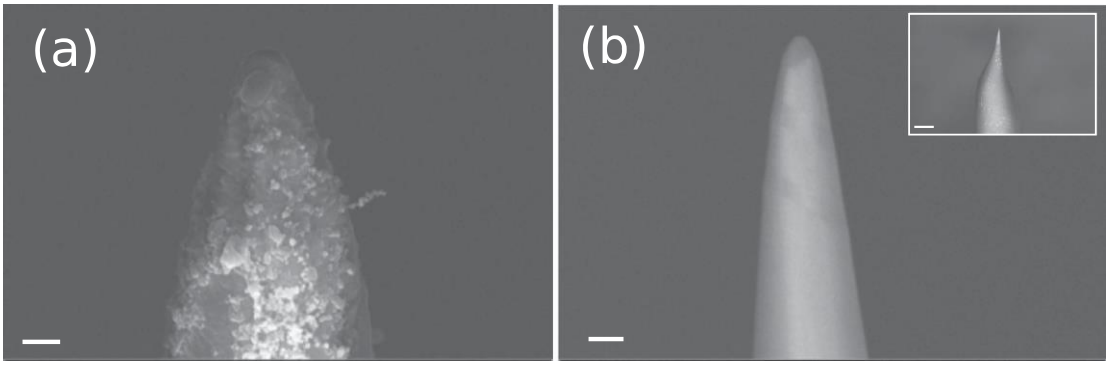


A 1. (a) A silver tip after the electrochemical etching steps at 20 000× magnification. The white scale bar is 400 nm. (b) The finished tip after the FIB milling at 75 000× magnification with a scale bar of 100 nm. The inset shows the whole tip at 300× magnification, with a scale bar of 40 $\mu$m. The final tip radius is approximately 20 nm.

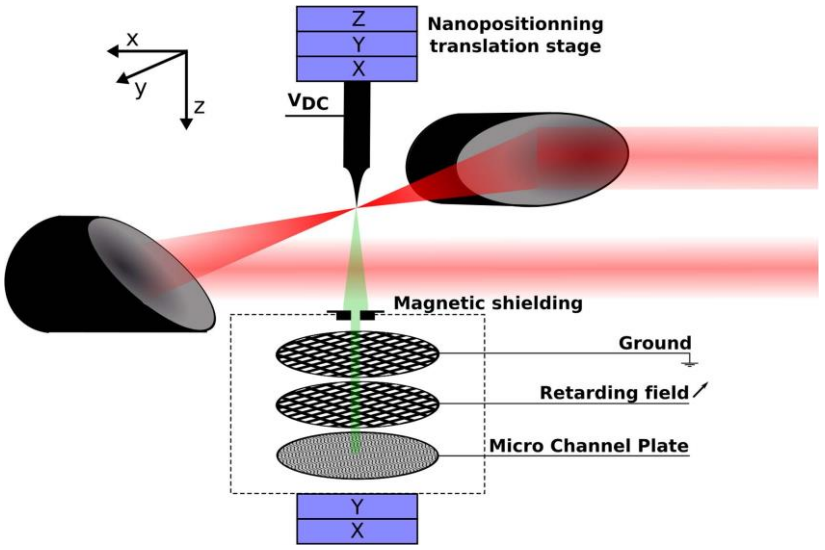


Figure B1. Experimental setup: the silver nanotip is illuminated by tightly focused femtosecond laser pulses with an additional tip bias $V_{DC}$. Electrons are detected by a field retarding spectrometer positioned in front of the tip apex.

## Appendix B. Photoemission experimental setup

A sketch of the experiment is depicted in figure B1. Femtosecond laser pulses are tightly focused onto the apex of a silver nanotip. We have used several laser sources. The first two, $S_1$ and $S_2$ are centered at 800 nm and share similar parameters (beam size and pulse duration). $S_1$ has a low repetition rate of 1 kHz while $S_2$ is at 62 MHz. Finally, we also used frequency-doubled pulses from $S_1$. The laser intensity is controlled with a half-wave plate polarizer energy throttle and the polarization is cleaned by a second polarizer, regulated by another half-wave plate and set along the tip axis for maximum photoemission when illumnating the apex. The laser beam is focused by an off-axis aluminum parabolic mirror with a focal length of 15 mm leading to a focal spot size of about 4 $\mu$m and optical intensities on the order of $10^{12}$ W cm$^{-2}$. The experiment is performed in a stainless steel ultra-high vacuum chamber with a pressure on the order of $10^{-10}$ mbar. A metal-plate with a 500 $\mu$m pinhole is placed $\sim$7 mm from the apex of the tip to define a ground potential and an additional DC voltage between 0 and 600 V is applied to the tip (hereafter referred to as $V_{DC}$).A field retarding spectrometer based on a mesh grid with an adjustable voltage combined with a double stage micro channel plate measures the kinetic energy distribution of the electrons with an estimated resolution of $DE/E \gg 5 \times 10^{-3}$. The spectrometer is placed in a magnetic shield to isolate low-energy electrons from external magnetic fields. The spectrometer is mounted on XY translation stages as well, in order to map the spatial distribution of the emitted electrons and align the spectrometer such that only electrons from the apex of the tip are measured. Alignment of the tip into the laser focus is achieved using three-dimensional nano-positioning translation stages (from Attocube systems

AG) with sub-micrometer resolution and a range of a few millimeters. The alignment is checked by imaging the nanotip on a CCD camera with a second parabolic mirror recollimating the beam and sending it out of the chamber. We use cold-field emission and Fowler–Nordheim plots [27] to measure the static field enhancement $b = E_{DC}/V_{DC}$, where $E_{DC}$ is the static electric field at the apex of the tip. Using the method described in [27], we can confirm the measurement of the tip radius from SEM images and we find $\beta \approx 4 \times 10^6$ m$^{-1}$. When recording laser-induced emission, the kinetic energy acquired from the applied $V_{DC}$ (typically 50 V) is subtracted from the recorded spectra.

## References


[1] Hommelhoff P, Sortais Y, Aghajani-Talesh A and Kasevich M A 2006 *Phys. Rev. Lett.* 96 1
[2] Ropers C, Solli D R, Schulz C P, Lienau C and Elsaesser T 2007 *Phys. Rev. Lett.* 98 1
[3] Kruger M, Schenk M and Hommelhoff P 2011 *Nature* 475 78
[4] Herink G, Solli D R, Gulde M and Ropers C 2012 *Nature* 483 190
[5] Piglosiewicz B, Schmidt S, Park D J, Vogelsang J, Groß P, Manzoni C, Farinello P, Cerullo G and Lienau C 2013 *Nat. Photon.* 8 37
[6] Juffmann T, Klopfer B B, Skulason G E, Kealhofer C, Xiao F, Foreman S M and Kasevich M A 2015 *Phys. Rev. Lett.* 115 264803
[7] Feist A, Echternkamp K E, Schauss J, Yalunin S V, Schäfer S and Ropers C 2015 *Nature* 521 200
[8] Ehberger D, Hammer J, Eisele M, Krüger M, Noe J, Högele A and Hommelhoff P 2015 *Phys. Rev. Lett.* 114 227601
[9] Gulde M, Schweda S, Storeck G, Maiti M, Yu H K, Wodtke A M, Schäfer S and Ropers C 2014 *Science* 345 200
[10] Barwick B, Corder C, Strohaber J, Chandler-Smith N, Uiterwaal C and Batelaan H 2007 *New J. Phys.* 9 142
[11] Bionta M R, Chalopin B, Champeaux J P, Faure S, Masseboeuf A, Moretto-Capelle P and Chatel B 2014 *J. Mod. Opt.* 61 833
[12] Bormann R, Gulde M, Weismann a, Yalunin S V and Ropers C 2010 *Phys. Rev. Lett.* 105 1
[13] Kealhofer C, Foreman S M, Gerlich S and Kasevich M A 2012 *Phys. Rev.* B 86 1
[14] Bionta M R, Chalopin B, Masseboeuf A and Chatel B 2015 *Ultramicroscopy* 159 Pt 2 152
[15] Swanwick M E, Keathley P D, Fallahi A, Krogen P R, Laurent G, Moses J, Kärtner F X and Velásquez-García L F 2014 *Nano Lett.* 14 5035
[16] Zhang C, Gao B, Chen L G, Meng Q S, Yang H, Zhang R, Tao X, Gao H Y, Liao Y and Dong Z C 2011 *Rev. Sci. Instrum.* 82 083101
[17] Sasaki S S, Perdue S M, Perez A R, Tallarida N, Majors J H, Apkarian V A and Lee J 2013 *Rev. Sci. Instrum.* 84 096109
[18] Miller M K and Russell K F 2007 *Ultramicroscopy* 107 761
[19] Krausz F and Ivanov M 2009 *Rev. Mod. Phys.* 81 163
[20] Krüger M, Schenk M, Hommelhoff P, Wachter G, Lemell C and Burgdörfer J 2012 *New J. Phys.* 14 0850019
[21] Thomas S, Krüger M, Förster M, Schenk M and Hommelhoff P 2013 *Nano Lett.* 13 4790
[22] Winsemius P, van Kampen F F, Lengkeek H P and van Went C G 1976 *J. Phys. F: Met. Phys.* 6 1583
[23] Babar S and Weaver J H 2015 *Appl. Opt.* 54 477
[24] Thomas S, Wachter G, Lemell C, Burgdörfer J and Hommelhoff P 2015 *New J. Phys.* 17 063010
[25] Arbouet A, Houdellier F, Marty R and Girard C 2012 *J. Appl. Phys.* 112 53103
[26] Houdellier F, Masseboeuf A, Monthioux M and Hÿtch M J 2012 *Carbon* 50 2037
[27] Gomer R 1961 *Field Emission and Field Ionization* vol 34 (Cambridge, MA: Harvard University Press )